A Numerical Study of Nonlinear Instability Phenomena in Solid Rocket Motors

Jay N. Levine*
Air Force Rocket Propulsion Laboratory/DYC, Edwards AFB, California
and
Joseph D. Baum†
University of Dayton, Dayton, Ohio

An existing nonlinear instability model has been extended and improved to allow it to more realistically treat the longitudinal shock-wave type of combustion instability frequently encountered in tactical solid rocket motors. Results obtained utilizing this model to investigate limiting amplitude and velocity-coupling phenomena in solid rocket motors are presented. An advanced finite difference integration technique capable of accurately describing shocks and contact discontinuities has been incorporated into the computer program, as well as an improved heat conduction solution, an heuristic velocity-coupling model, and a spectral analysis capability. Solutions demonstrating that limiting amplitude is independent of the characteristics of the initial disturbance are presented, as are results of a preliminary study of nonlinear velocity coupling demonstrating such phenomena as triggering, mean pressure shift, modulated limit cycles, and threshold velocity effects.

Nomenclature

A,B = transient burning rate parameters
c_p = specific heat of gas at constant pressure
c_s = specific heat of solid propellant
H = nondimensional surface heat release parameter
k = thermal conductivity
n = pressure exponent in steady-state burn rate law
P = pressure
Q_s = net heat of reaction for processes at burning surface
r = burn rate
T = temperature
u = velocity
W = mass burning rate, per unit length, per unit cross-sectional area
x = axial distance
ρ = density
κ = thermal diffusivity
Ω = nondimensional frequency, $\omega\kappa/\bar{r}^2$

Subscripts

g = gas
pc = pressure coupled
s = at the burning surface
vc = velocity coupled

Superscripts

$(\ )'$ = a perturbation
$(\bar{\ })$ = steady-state value

Introduction

NONLINEAR axial mode instability in solid-propellant rocket motors is initiated by random finite amplitude events such as the expulsion of an igniter or insulation fragment through the nozzle. When instability is initiated in this manner in a motor that is otherwise linearly stable (i.e., stable to infinitesimal disturbances) it is said to be a "triggered" instability. The existence of triggered instabilities is a direct result of the fact that all of the acoustic energy gain or loss mechanisms in a solid rocket motor, e.g., pressure and velocity coupled driving, nozzle and particle damping, acoustic mean flow interactions, etc., are nonlinear, i.e., amplitude dependent to some degree. These same nonlinearities also ensure that a nonlinear instability will not grow without limit, but rather will eventually reach a limit cycle amplitude at which the net gains and losses are balanced.

Nonlinear axial mode instabilities usually result in pressure oscillations that propagate as steep-fronted waves which are actually weak shock waves. The acoustic pressure and velocity oscillations are frequently accompanied by an increase in mean chamber pressure (usually referred to as a dc shift) and increased mean propellant burn rate. This increased burn rate is thought to be primarily a response to acoustic velocity oscillations; thus, it is often referred to as acoustic erosivity.

Certain trends and characteristics of nonlinear instability have been documented. However, attempts to form generally applicable conclusions have been stymied by the number and complexity of mutual interactions between the governing physical phenomena. The ability to predict, avoid, or eliminate nonlinear instability is, therefore, clearly contingent upon our ability to understand and model these phenomena.

Efforts to understand and model nonlinear instability date back to the 1960s, e.g., Refs. 1-3. The most recent work has been divided between so-called "exact" and "approximate" mathematical approaches. The "exact" methods of Levine and Culick[4] and Kooker and Zinn[5] seek to numerically solve the nonlinear partial differential equations governing both the mean and time-dependent flow in the combustion chamber, as well as the combustion response of the solid propellant. The "approximate" methods of Culick[6] and Powell et al.[7] utilize expansion techniques to reduce the problem to the solution of sets of ordinary differential equations. Culick and Levine[8] carried out a brief comparison of results obtained with these two approaches and found that within certain limits the approximate techniques yield quite reasonable results. Each of these methods has certain advantages, disadvantages, and limitations with regard to accuracy, computation time, generality, etc.

The previously developed "exact" and "approximate" nonlinear instability programs are not capable of treating the multiple traveling shock-wave type of instability that occurs in

Presented as Paper 81-1524 at the AIAA/SAE/ASME 17th Joint Propulsion Conference, Colorado Springs, Colo., July 27-29, 1981; submitted Aug. 14, 1981; revision received April 3, 1982. This paper is declared a work of the U.S. Government and therefore is in the public domain.

*Research Physical Scientist.
†Research Scientist, Research Institute; presently with the Air Force Rocket Propulsion Laboratory/DYC, Edwards AFB, Calif. Member AIAA.

the reduced and minimum smoke motors that have since been developed. Nor did these analyses contain a model for velocity coupling; something which appears to be required in order to predict the types of triggering events and dc pressure shifts that have been observed. The objective of the present research is to extend and improve the model developed in Ref. 4 to the point where it can be used as a tool to enhance our understanding of nonlinear instability, as a means to aid in the design and interpretation of related experimental work; as a means to evaluate the validity of advanced combustion response models, and as a design aid to solve or prevent nonlinear instability problems.

In order to reach the stated objective, the numerical techniques utilized in Ref. 4 had to be replaced by more advanced methods and a model for addressing velocity-coupled effects had to be incorporated into the computer program. Other improvements, such as the ability to spectrally analyze the computed waveforms, have also been accomplished.

A critical investigation of the ability of finite difference integration methods to accurately solve the one-dimensional, nonlinear, two-phase, hyperbolic equations which govern the propagation of shock waves in combustion chambers was conducted.[9] The results of this investigation showed that excellent results are obtained by employing a combination operator consisting of the Lax-Wendroff scheme[10] hybridized with Harten and Zwas' first-order scheme[11] and further modified by an artificial compression correction.[12]

The capability of the present model to accurately predict the propagation of multiple shock waves in variable cross-sectional area rocket chambers was demonstrated in Ref. 13. The model predicts the tendency of motors with area discontinuities to form multiple shock waves, a tendency that has been confirmed experimentally (e.g., Ref. 14). The solutions obtained also demonstrated the complex axial variation in pressure oscillation spectra that can be expected in variable cross-sectional area motors.

The sensitivity of solid propellants to acoustic velocity oscillations parallel to the burning surface has been known for many years. This phenomenon, termed velocity coupling, has been observed in both motors and laboratory burners. These observations also support the hypothesis that velocity coupling can be highly nonlinear, and that it is the most likely cause of triggered instabilities and mean pressure shifts in solid rockets. The development of a new model for velocity coupling was not considered to be part of the present investigation. Rather, existing models were reviewed to determine which, if any, should be incorporated into the analysis at this time.

The objective of this paper is to present some of the interesting results obtained with the extended nonlinear combustion instability model, including the effect of initial disturbance amplitude and waveform, combustion response, and particle concentration upon limiting amplitude; and the ability of ad hoc velocity-coupling models to predict phenomena such as triggering and mean pressure shifts.

Limiting Amplitude Studies

From a practical standpoint, the ability to predict the limiting amplitude reached by pressure oscillations in unstable solid rocket motors is important in assessing whether such an instability will be severe enough to warrant design or propellant modifications to eliminate it. For both practical and theoretical reasons it is also important to establish whether limit cycles are unique, i.e., independent of the characteristics of the initiating disturbance.

Even under the most carefully controlled laboratory conditions, it is almost impossible to conduct a series of motor firings in which the only variable is either initial disturbance amplitude or waveform. To the authors' knowledge no test series having the primary purpose of establishing the effect of initial disturbance on limiting amplitude has ever been conducted. Results obtained from some tests which approximate the required conditions are not definitive; however, on balance they favor a conclusion that limiting amplitude is independent of the initiating disturbance. It should be emphasized that the above refers to the limit amplitude reached if a motor is pulsed into instability. The fact that the triggering event itself is dependent on pulse characteristics has been clearly demonstrated.

The difficulty in experimentally examining the uniqueness of limit cycles makes the analytical examination of this question all the more important. The question has been previously addressed for both liquid[15,16] and solid[4,6,7,9] rocket motors using both expansion and numerical techniques. Results obtained from expansion solutions indicate that the limit cycle should be independent of the initiating disturbance. However, since these methods have limits in regard to their applicability to strongly nonlinear situations with very high amplitudes and/or steep-fronted shock-type waveforms, and since not all of the nonlinearities present in tactical solid rocket motors were incorporated in the models, the conclusions must be regarded as relevant but requiring further substantiation.

Previous results obtained with the present "exact" model seemed to yield apparently conflicting conclusions. Results obtained in Ref. 4, for motors with a particle-to-gas weight flow ratio of 0.36 and 2 μm particles, appeared to demonstrate that limiting amplitude is a strong function of initial disturbance amplitude. Conversely, solutions obtained for almost identical conditions, but without particles,[9] yielded the same limiting amplitude for both standing wave- and pulse-type initial disturbances of widely varying amplitudes. It was tentatively concluded that the apparently conflicting results were due to nonlinear particle damping effects. Since this previous conclusion was based on a limited number of results it was decided to obtain several more sets of solutions, with and without particles. In this connection, it should be mentioned that this investigation addresses the question of limiting amplitude for linearly unstable motor/propellant combinations (i.e., motor/propellant combinations that under the specific motor operating conditions are unstable to infinitesimal pressure oscillations). In such cases, limit cycles result from the amplitude dependence (nonlinear behavior) of the operative driving and damping mechanisms.

The nonlinear transient burn rate model utilized here[4] is a nonlinear extension of the Denison and Baum model.[17] Similar models (except for some subtle differences) were developed by Krier et al.[18] and Kooker and Zinn.[5] The two most important assumptions employed in the model are: the gas and solid phase are treated as homogeneous; and the gas phase responds in a quasi-steady manner. The model utilized reduces to the Denison and Baum model in the linear limit. In this connection, it should be mentioned that the pressure- and velocity-coupled response function (R_{pc} and R_{vc}, respectively) values specified in this paper are equivalent linear response function values (i.e., obtained by reducing the nonlinear model to the linear limit). These values are given for comparison purposes only. In the program, the instantaneous local burn rate is evaluated utilizing the nonlinear transient burn rate model.

The series of results shown in Fig. 1 are for a cylindrically perforated motor 59.7 cm (23.5 in.) long with a port area of 21.484 cm^2 (3.33 in.^{2}) a throat area of 2.8322 cm^2 (0.439 in.^{2}) and a chamber pressure of 13.19 MPa (1913 psi). These calculations were performed for a propellant without particles, with a linear pressure-coupled response function of 5.35 and with no velocity coupling. The solutions were initiated by perturbing the steady state with fundamental mode disturbances of varying amplitudes. The calculated pressure perturbation histories at the head end of the motor are shown for initial amplitudes of 40, 8, and 2% of the mean pressure. Other solutions were also obtained for amplitudes of 60 and 10% of the mean pressure. All of the solutions

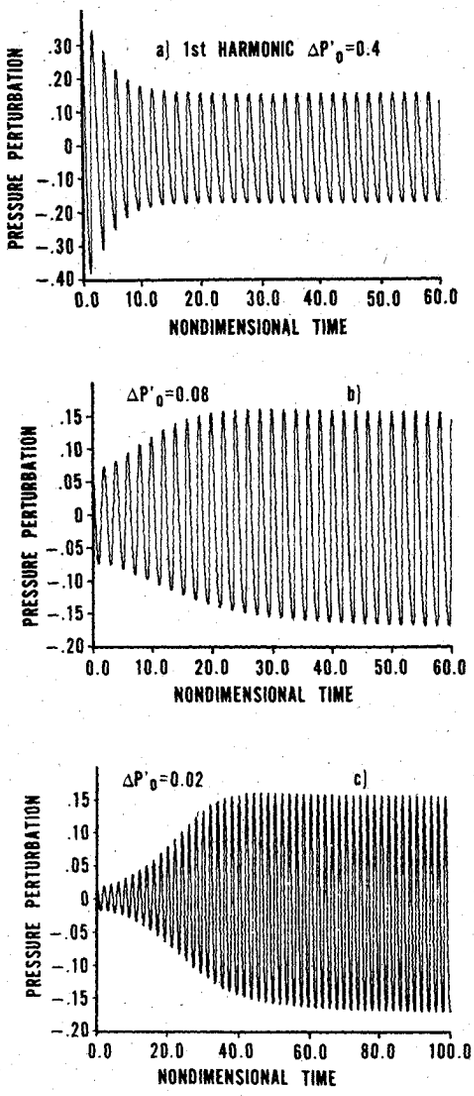

Fig. 1 Time evolution of pressure oscillations at the head end of the motor (no particles).

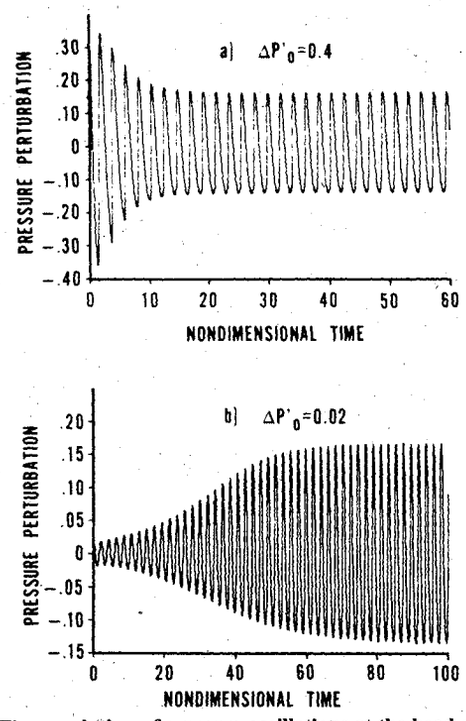

Fig. 2 Time evolution of pressure oscillations at the head end of the motor (15%, 2 μm particles).

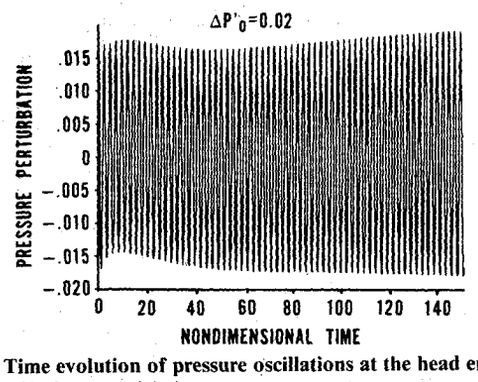

Fig. 3 Time evolution of pressure oscillations at the head end of the motor (36%, 2 μm particles).

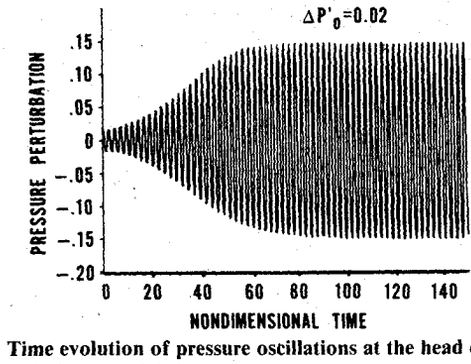

Fig. 4 Time evolution of pressure oscillations at the head end of the motor (36%, 2 μm particles).

reached the same limiting amplitude, 32.7% of the mean pressure (peak to peak).

Additional solutions for the same motor and operating conditions were obtained with several other pressure-coupled response functions. All of the solutions for a given response function reached the same limiting amplitude, but each response function produced a different limiting amplitude.

Several other series of calculations were then performed with varying sizes and amounts of particles to re-examine the conclusion reached in Ref. 4. The first series of calculations (with the same motor geometry used in the results shown in Fig. 1) was conducted with 2 μm aluminum oxide particles and 15% particle-to-gas weight flow ratio. The results shown in Fig. 2 were enlightening. The computed limit cycle amplitudes were the same (30.4% of mean pressure, peak to peak) even though the initial disturbance was 40% in one case and 2% in the other. Calculations with intermediate initial disturbances also reached the same limit amplitude.

This last series of results raised serious questions concerning the validity of the conclusion reached in Ref. 4. In order to settle the apparent conflict, the earlier solutions were recalculated. This time, however, the solutions were carried out for twice as many wave cycles. Doing so immediately provided the answer to this seeming paradox. At a nondimensional time of 70 (when the earlier solutions were terminated) the decay rate was quite small, but not zero. It was falsely assumed that continuing the solutions would not significantly alter the limit cycle amplitudes. The present calculations show that except for initial perturbations close to 5%, the wave is either still growing or decaying at $T=150$. All of the solutions were getting closer and closer to the same limiting amplitude, but had yet to reach it. Figure 3 shows the present results obtained with 2 μm particles, 36% particle-to-gas weight flow ratio and an initial disturbance amplitude of 2% of the mean pressure. This figure demonstrates that when

a particular motor/propellant combination is near neutral stability (i.e., very small growth or decay rate), a very long time is needed to reach a limit cycle condition.

To further demonstrate the effect of relative stability on the time needed to reach a limit cycle condition, calculations were made for the same motor and propellant (36% of 2 μm particles), but with an increased pressure-coupled response function. The increased combustion driving unbalances the gains and losses, and as seen in Fig. 4, results in the relatively rapid establishment of a limit cycle with an amplitude of 29.6% of the mean pressure. Here again, additional solutions demonstrated that limit cycle amplitude was independent of initial disturbance amplitude.

Velocity Coupling

A survey of past attempts to model or predict the effects of velocity coupling on the stability of solid rocket motors leads one to the conclusion, supported by the results of a recent JANNAF workshop on velocity coupling,[19] that very little is known about velocity coupling at this time. All existing models appear to have significant deficiencies. Price's original velocity-coupling model[20] is purely empirical. Other investigators sought to modify existing combustion models by introducing an additional source of heat transfer to the propellant surface. For example, in Refs. 21 and 22, a heat-transfer term based on an empirical function of velocity was utilized, while in Refs. 23-25, additional heat transfer was included on the basis of modifications to steady-state turbulent boundary-layer theories and/or erosive burning rate models. All of these models ignore some of the fundamental physics of the problem. Turbulent boundary layers in the usual sense are not typically realized in solid rocket motor chambers.[26] While some of the existing velocity-coupling models properly reduce to steady-state erosive burning models as the limit of zero frequency is approached, none of them properly treat acoustic boundary-layer effects that become significant in the normal longitudinal frequency range[27] (approximately 200-1000 Hz). In addition, acoustic boundary-layer transition and acoustic turbulence interactions may also be important under certain conditions, as may the interaction of an unsteady boundary layer with the propellant surface structure.

Due to the deficiencies of currently existing models, no velocity-coupling model was selected for incorporation into the overall nonlinear stability program at this time. Instead, calculations were performed utilizing several different ad hoc functions of velocity to directly augment either the heat transfer to the propellant surface or the transient burning rate itself.

The primary purpose of this velocity-coupling study was to demonstrate the potential usefulness of the present analytical framework in assessing the validity of improved velocity-coupling models as they are developed. The initial calculations to be presented herein are for constant cross-sectional area, cylindrically perforated motors. The basic configuration is the same as that used in the previous studies.[4,9] The reasons for selecting a cylindrical configuration to start with were: 1) it was the simplest possible motor configuration; 2) a large body of pressure coupled only solutions was available for these configurations; 3) linear velocity coupling theory[28] yields no effect of velocity coupling for such configurations, thus, any velocity coupling effects observed would be due to nonlinear effects; and 4) although cylindrical motors often show little evidence of velocity coupling, there are many recorded instances where severe triggered instabilities, with large mean pressure shifts have been observed in such motors.[1-3,14]

All of the velocity-coupling models developed to date have retained Denison and Baum's assumption of quasi-steady gas-phase behavior in the combustion zone above the propellant surface. Each of the models then makes certain assumptions and hypothesis that lead to a velocity-dependent term that enhances the heat transfer from the combustion zone to the propellant surface. In terms of the combustion model which is currently utilized in the present nonlinear analysis, this corresponds to incorporation of an additional term in the surface energy balance.

Symbolically, this equation may be written as

$$K_g \frac{\partial T}{\partial x}\bigg|_- = K_g \frac{\partial T}{\partial x}\bigg|_+ + \rho_s r Q_s \qquad (1)$$

heat transfer to solid propellant | heat transfer from gas phase to surface | total energy released at surface

The term $K_g(\partial T/\partial x)\,|_+$ has to be modified to incorporate the effect of acoustic velocity fluctuations. In the absence of a fundamental physical model, a number of functional forms were considered. Since a functional form of the following type has sometimes been successful in rationalizing observed events, it was considered first

$$\left[K_g \frac{\partial T}{\partial x}\bigg|_+\right]_{vc} \approx \left[\epsilon_1(|u|-u_t)-\epsilon_2(\bar{u}-u_t)\right]$$

where

$$\epsilon_1 = \begin{bmatrix} 0, & |u| < u_t \\ 1, & |u| > u_t \end{bmatrix} \qquad \epsilon_2 = \begin{bmatrix} 0, & \bar{u} < u_t \\ 1, & \bar{u} > u_t \end{bmatrix} \qquad (2)$$

Here u is the total velocity, $u=\bar{u}+u'$; $\bar{u}$ is the mean velocity; and u' the local velocity fluctuation. The term u_t represents a threshold velocity which in reality may or may not exist. Justification for this functional form may be found in several references.[20,21]

When $u' \gg \bar{u}$ and $u_t = 0$, Eq. (2) can be approximated by

$$\left[K_g \frac{\partial T}{\partial x}\bigg|_+\right]_{vc} \approx |u'| \qquad (3)$$

According to linear analysis, a term such as shown in Eq. (2) can only be added to the heat transfer. However, in nonlinear analysis a velocity-coupled heat-transfer term can be incorporated on an additive or multiplicative basis. It was decided to insert a term on a multiplicative basis. The following functional form was adopted:

$$\left[K_g \frac{\partial T}{\partial x}\bigg|_+\right]_{pc+vc} = \left[K_g \frac{\partial T}{\partial x}\bigg|_+\right]_{pc}\left[1+\frac{R_{vc}}{R_{pc}}\theta_{vc}F(u)\right] \qquad (4)$$

Where $F(u)$ is given by Eqs. (2) or (3), R_{pc} is the pressure-coupled response function and R_{vc} is the velocity-coupled response function.

For small-amplitude oscillations, $u' < \bar{u}$ and $u_t = 0$, the right-hand side of Eq. (2) reduces to u'. Thus, using the combustion model evaluated in the linear limit,[4] it can be shown that for R_{vc} to be equal to R_{pc}, θ_{vc} in Eq. (4) must satisfy

$$\theta_{vc} = \left[2n(1-H)+\frac{C_p(n-n_s)}{C_s A}\right]\Big/(1-H) \qquad (5)$$

In the small-amplitude linear limit, Eq. (4), combined with the present combustion model, reduces to the velocity-coupled model used by Culick[21] and Levine and Culick.[22] Equations (4) and (5), together with either Eqs. (2) or (3), were termed the heat-transfer augmentation model.

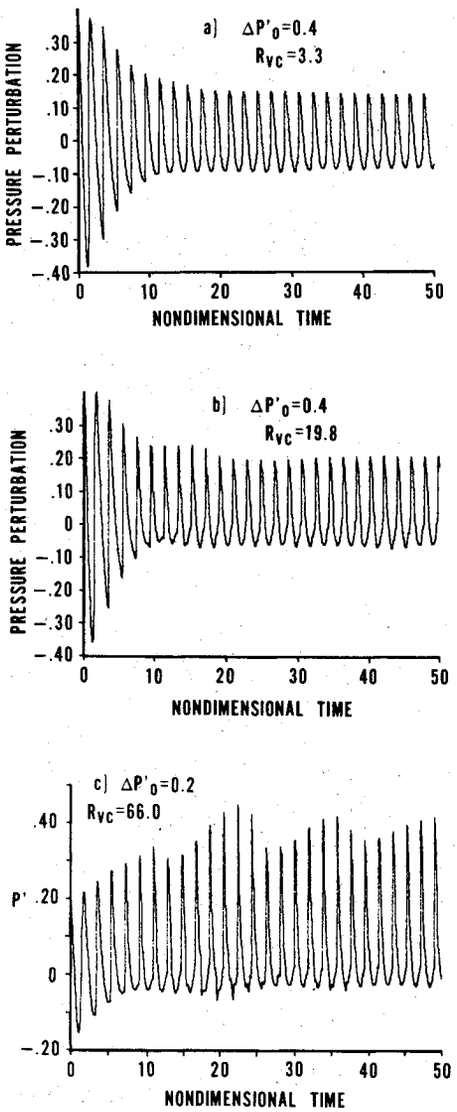

Fig. 5 Time evolution of pressure oscillations at the head end of the motor, velocity coupling augmenting the heat transfer to the propellant surface.

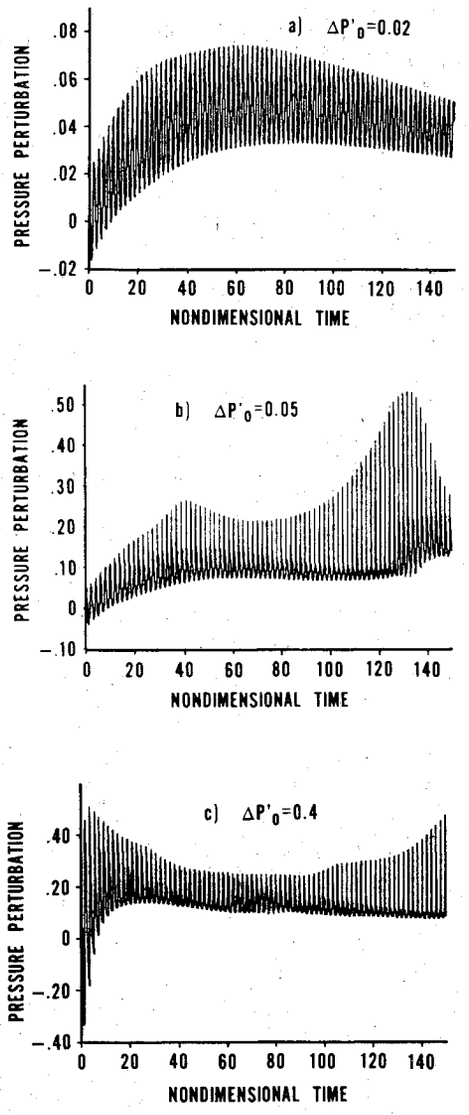

Fig. 6 Time evolution of pressure oscillations at the head end of the motor, burn rate augmentation model [$F(u)=|u'|$, $R_{vc}=5.01$, $R_{pc}=2.18$].

The calculations shown in Fig. 5 are for the same motor used in the Ref. 9 studies. With a pressure-coupled response function of 3.3 and no velocity coupling, this motor/propellant combination reached a limit amplitude of 21.73% of the mean pressure, peak to peak. With the heat-transfer augmentation model [Eqs. (2)], $u_t=0$ and a velocity-coupled response function of 3.3, the calculated waveform (Fig. 5a) is almost the same as with pressure coupling alone. At the limit cycle condition, the lower envelope of the oscillations is almost the same. However, the zero-to-peak amplitude was increased by 1.2%. Increasing the velocity-coupled response function to 19.8 gave the results shown in Fig. 5b. Here again, the lower envelope of the oscillations at the limit cycle remained at the same level, while the zero-to-peak amplitude was increased by 7.3%. Neither of these two cases demonstrated a measurable mean pressure shift, even after 75 wave cycles.

In order to further explore the reasons for this behavior, additional solutions were obtained with extremely high values of R_{vc}. At a value of $R_{vc}=40$, strong nonlinear effects and a measurable dc shift were produced. At $R_{vc}=66$ (Fig. 5c), a significant dc pressure shift is observed, as well as a modulated limit cycle amplitude.

In order to explore the ineffectiveness of the heat-transfer augmentation model, a second ad hoc velocity coupling formulation was inserted into the nonlinear instability analysis, as follows:

$$W_{pc+vc}=W_{pc}[1+R_{vc}F(u)] \tag{6}$$

where W is the instantaneous propellant mass burning rate ($W=\bar{W}+W'$) and W_{pc} the instantaneous mass burn rate computed from the existing pressure-coupled model. With $F(u)$ given by Eqs. (2), Eq. (6) also reduces in the low-amplitude limit to the linear velocity-coupling model used in the past. The key difference between Eqs. (6) and (4) is that the velocity-coupling effect built into Eq. (6) directly modifies the propellant burning rate rather than affecting it indirectly through a model that was developed for the pressure-coupled response function prediction. Equation (6), termed the burn rate augmentation model, is heuristic and is not meant to imply a particular physical velocity-coupling mechanism. However, it was felt that solutions obtained using it would be instructive.

A series of calculations were carried out with velocity coupling added on the basis of Eq. (6) with $F(u)=|u'|$, $R_{vc}=5$, and $R_{pc}=2.18$. The results obtained with pressure coupling only indicate that this motor/propellant combination is stable even to high-amplitude disturbances (these results are confirmed by linear theory analysis[28]). However,

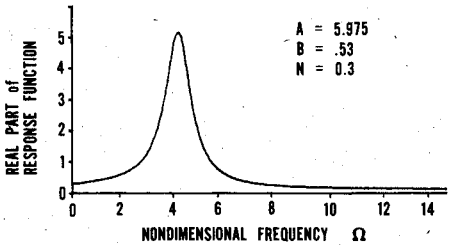

Fig. 7 Real part of response function vs frequency.

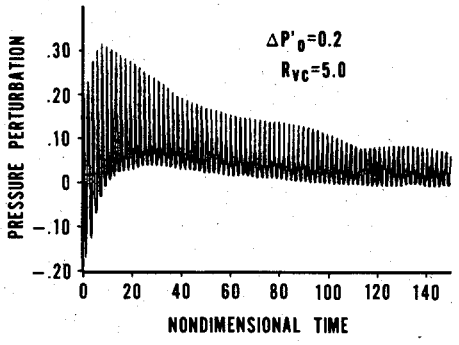

Fig. 8 Time evolution of pressure oscillations at the head end of the motor, burn rate augmentation model [$F(u)$ given by Eqs. (2)].

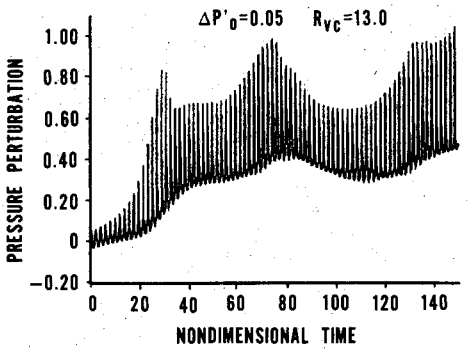

Fig. 9 Time evolution of pressure oscillations at the head end of the motor, burn rate augmentation model [$F(u)$ given by Eqs. (2)].

when both pressure and velocity coupling are included, the results are entirely different. With an initial disturbance amplitude of 2% (Fig. 6a), the disturbance amplitude grows initially, but the overall result indicates a stable motor. With a 5% initial disturbance (Fig. 6b), the oscillations grow to an amplitude of about 20% of the mean pressure (peak to peak), appear to start damping, but then grow again. A mean pressure shift of about 12% is observed. With a 40% initial disturbance (Fig. 6c) the disturbance amplitude decays until it reaches about 15% of the mean pressure, maintains that level for a while, and then begins to grow again. The mean pressure shift observed is about the same as that resulting from a 5% disturbance.

This last series of calculations demonstrates a number of characteristics of observed nonlinear instabilities; characteristics that the model with pressure coupling alone has not been able to simulate. These characteristics are triggering (Fig. 6a compared to Figs. 6b and 6c), waves that grow and then decay (Fig. 6b), mean pressure shifts that appear to be relatively independent of initial amplitude (Figs. 6b and 6c), and a lack of a stable limit cycle behavior, i.e., modulating amplitude (Figs. 6b and 6c). To the authors' knowledge, this is the first time such solutions have been obtained.

Based on these results, it has been concluded that the relative ineffectiveness of the heat-transfer augmentation model is a result of the response function vs frequency characteristics implied by the Denison and Baum type of model utilized. With such a quasi-steady combustion model, the gas-phase heat transfer (whether from pressure- or velocity-coupled effects) produces a response function vs frequency curve that has a single narrow peak. Figure 7 depicts the real part of the response function vs frequency curve for the parameters used in the calculations shown in Figs. 5, 6, and 8-10, (A=5.975, B=0.53). At the nondimensional frequency implied by the propellant burn rate parameters and motor operating conditions used in the calculations ($\Omega=3.78$) the linear pressure-coupled response function was equal to 3.3. At the second harmonic frequency ($\Omega=7.56$) the linear pressure-coupled response function is only 0.3, while at the higher harmonics it is even lower. With the heat-transfer augmentation model the velocity-coupled response function is, to first order, proportional to the pressure-coupled response. (Note: for the problems being considered, the waves are primarily traveling rather than standing, and the velocity is approximately in phase with the pressure over half the cycle and 180 deg out of phase with the pressure over the other half of the cycle.) Thus, for the problem that was solved, the velocity-coupled response for the second harmonic was about a factor of 10 lower than the response function at the fundamental frequency.

With the burn rate augmentation model [Eq. (6)] the velocity-coupling response is independent of the combustion model and, to first order, is independent of frequency. Thus, when a velocity-coupled response function of 5 was specified, this was the approximate value at all frequencies. Given the nature of Fig. 7, it would require a value of $R_{vc}/R_{pc}=16.6$ (which implies $R_{vc}=55$ for the first harmonic) in order for the heat-transfer augmentation model to produce a similar value of $R_{vc}=5$ for the second harmonic.

The above discussion appears to be able to explain the wide disparity between the results obtained with the two ad hoc models. Furthermore, it implies that a realistic velocity-coupling model will have to be capable of providing strong driving at the higher harmonic frequencies.

In order to examine the effect of $F(u)$ on the computed results, $|u'|$ was replaced by Eqs. (2), and the same series of calculations were repeated. Figure 8 shows the calculated results for an initial amplitude of 20%. In this case the motor appears to be marginally stable. To examine the behavior induced by Eqs. (2) under unstable conditions, the calculations were repeated with a velocity-coupled response function (R_{vc}) equal to 13. Even with such a large velocity-coupled response, a stable solution was obtained with an initial disturbance amplitude of 2%. Increasing the initial disturbance amplitude to 5% (Fig. 9), however, produced a large-amplitude, highly modulated instability with a significant mean pressure shift.

The sensitivity of the results to the functional form of the velocity perturbation indicates that the present nonlinear stability analysis can be useful in assessing the validity of more realistic velocity-coupling models, as they are developed.

To further our understanding of the velocity-coupling problem and nonlinear instability in general, the solutions presented in Figs. 6a and 6c were examined in detail[29]; not only at the head and aft ends but also at the one-quarter, one-half, and three-quarter points. Examination of the phase angles between the pressure, velocity and burn rate oscillations indicated a very complex behavior that is, undoubtedly, a result of many mutually interacting nonlinear fluid dynamic and combustion phenomena. The analysis showed that the waves are primarily, but not completely, traveling waves, even when the waves were not steep fronted or when the waves were of relatively low amplitude. The frequency content of the waves and the phase relationships of the pressure, velocity, and burning rate vary significantly from one point in the motor to another, and for the same

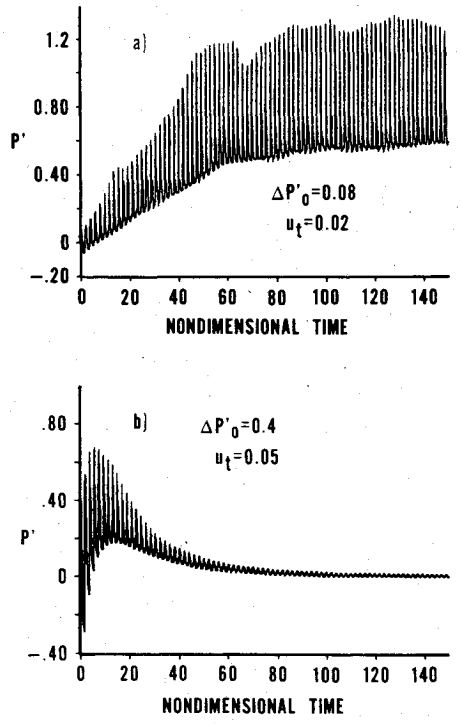

Fig. 10 Time evolution of pressure oscillations at the head end of the motor, burn rate augmentation model with threshold velocity, $R_{vc} = 13$.

motor vary as a function of the initial disturbance amplitude. In addition, the phase angles between w', u', and p' vary intracycle, i.e., from one portion of the wave cycle to another, and also vary in time from one cycle to another. This nonstationary behavior of the phase angles is the most likely cause of modulated limit cycle amplitudes that are observed in the nonlinear velocity-coupling solutions.

Threshold Effects

All of the velocity-coupling solutions previously presented herein were for zero threshold velocity. Since threshold effects have been observed,[30] a brief attempt was made to examine their effect within the context of the present ad hoc models. The results presented in Fig. 10 were obtained for the same motor used in the other cases presented herein. The burn rate augmentation model was utilized with $F(u) = |u'| - u_t$. With the pressure and velocity coupling values used in the Fig. 6 results ($R_{pc} = 2.18$, $R_{vc} = 5$) a threshold velocity equal to 0.02 (u_t is normalized by the steady-state gas sound speed so $u_t = 0.02$ corresponds to about 18.29 m/s or 60 ft/s) resulted in a stable solution. R_{vc} was then increased to 13 and the calculations were repeated. In this case, with $u_t = 0.02$ and $\Delta P = 0.02\bar{P}$, a stable result was again achieved. However, when ΔP was increased to $0.08\bar{P}$, a highly nonlinear instability was produced (Fig. 10a). The threshold velocity was then increased to 0.05. With the increased threshold velocity an unstable result could not be achieved, even with initial perturbations as large as 40% of the mean pressure (Fig. 10b).

Although threshold effects, if they exist, are not expected to be a function of only mean and/or fluctuating velocity, these results indicate that, as expected, threshold effects act to increase the magnitude of the velocity-coupled response function required to trigger an instability. The results also imply that propellants with high acoustic velocity thresholds will be difficult or impossible to trigger.

Conclusions

The complexity of nonlinear instability in solid-propellant rocket motors and the large number of mutually interacting physical phenomena which control it make it very difficult to form generally valid quantitative conclusions, even from a relatively large number of numerical or experimental results.

The following conclusions can, however, be drawn from the large number of nonlinear instability solutions obtained during the present investigation:

1) Based on many more solutions than had been available in the past, it is concluded that pressure oscillations will reach a limiting amplitude that is independent of the characteristics (waveform and amplitude) of the initiating disturbance. This conclusion appears to hold for unmetallized as well as metallized solid propellants, but cannot as yet be generalized to include cases when strong nonlinear velocity coupling is present (see conclusion 5).

2) Velocity-coupling models based on modifications to standard quasi-steady gas-phase and homogeneous solid-phase assumptions are not capable of producing strong nonlinear effects at realistic values of velocity-coupled response function.

3) A realistic velocity-coupling model must be capable of predicting high combustion response over a wide frequency range for propellants that are known to be able to produce strong nonlinear velocity coupling effects.

4) Nonlinear oscillations in solid rocket motors are very complex. The oscillations are, in general, a combination of traveling and standing waves, with the traveling component being dominant, even for non-steep-fronted waves at relatively low amplitudes.

5) The phase angles between pressure, velocity, and burning rate oscillations vary from one location in the motor to another and are nonstationary in time. The nonstationary behavior of the phase angles is the most likely cause of the modulated limit cycle amplitudes observed in the solutions and in motors.

6) The predicted results were quite sensitive to changes in both the magnitude of the velocity-coupled response function utilized and its functional dependence. Thus, it is concluded that the present comprehensive nonlinear stability analysis will prove to be valuable in assessing the validity of improved velocity-coupling models as they are developed.

7) Solutions obtained using a threshold velocity imply that propellants with high acoustic velocity thresholds will be difficult or impossible to trigger unless they also have a very high level of velocity-coupled response.

References

[1] Price, E.W., "Axial Mode Intermediate Frequency Combustion Instability in Solid Propellant Rocket Motors," AIAA Paper 64-146, Jan. 1964.

[2] Brownlee, W.G., "Nonlinear Axial Combustion Instability in Solid Propellant Motors," *AIAA Journal*, Vol. 2, Feb. 1964, pp. 275-284.

[3] Marxman, G.A. and Wooldrige, C.E., "Finite-Amplitude Axial Instability in Solid Rocket Combustion," *Proceedings of the Twelfth Symposium (International) on Combustion*, The Combustion Institute, Pittsburgh, Pa., 1969, pp. 115-127.

[4] Levine, J.N. and Culick, F.E.C., "Nonlinear Analysis of Solid Rocket Combustion Instability," AFRPL-TR-74-45, Oct. 1974.

[5] Kooker, D.E. and Zinn, B.T., "Numerical Investigation of Nonlinear Axial Instabilities in Solid Rocket Motors," BRL-CR-141, March 1974.

[6] Culick, F.E.C., "Nonlinear Behavior of Acoustic Waves in Combustion Chambers," *Proceedings of 10th JANNAF Combustion Meeting*, Vol. 1, CPIA Pub. 243, 1973, pp. 417-436.

[7] Powell, E.A., Padmanabahn, M.S., and Zinn, B.T., "Approximate Nonlinear Analysis of Solid Rocket Motors and T-Burners," AFRPL-TR-77-48, 1977.

[8] Culick, F.E.C. and Levine, J.N., "Comparison of Approximate and Numerical Analyses of Nonlinear Combustion Instability," AIAA Paper 74-201, Jan. 1974.

[9] Baum, J.D. and Levine, J.N., "Evaluation of Finite Difference Schemes for Solving Nonlinear Wave Propagation Problems in Rocket Combustion Chambers," AIAA Paper 81-0420, Jan. 1981.

[10] Lax, P.D. and Wendroff, B., "System of Conservation Laws" *Communications on Pure and Applied Mathematics*, Vol. 13, 1960, pp. 217-237.

[11] Harten, A. and Zwas, G., "Self Adjusting Hybrid Schemes for Shock Computations," *Journal of Computational Physics*, Vol. 9, 1972, pp. 568-583.

[12] Harten, A., "The Artificial Compression Method for Computation of Shock and Contact Discontinuities, III: Self Adjusting Hybrid Schemes," AFOSR-TR-77-0659, March 1977.

[13] Levine, J.N. and Baum, J.D., "A Numerical Study of Nonlinear Instability Phenomena in Solid Rocket Motors," AIAA Paper 81-1524, July 1981.

[14] Hughes, P.M. and Smith, D.L., "Nonlinear Combustion Instability in Solid Propellant Rocket Motors. Influence of Geometry and Propellant Formulation," Paper presented at 53rd AGARD Meeting, Propulsion and Energetics Panel, Oslo, Norway, April 1979.

[15] Zinn, B.T. and Powell, E.A., "Nonlinear Combustion Instability in Liquid Propellant Rocket Engines," *Proceedings of 13th Symposium (International) on Combustion*, The Combustion Institute, Pittsburgh, Pa., 1971, pp. 491-503.

[16] Powell, E.A. and Zinn, B.T., "The Prediction of Nonlinear Three-Dimensional Combustion Instability in Liquid Rockets with Conventional Nozzles," NASA CR-121279, Oct. 1973.

[17] Denison, M.R. and Baum, J.D., "A Simplified Model of Unstable Burning in Solid Propellants," *ARS Journal*, Vol. 31, Aug. 1961, pp. 1112-1122.

[18] Krier, H., T'ien, J.S., Sirignano, W.A., and Summerfield, M., "Nonsteady Burning Phenomena of Solid Propellants: Theory and Experiments," *AIAA Journal*, Vol. 6, Feb. 1968, pp. 278-285.

[19] Beckstead, M.W., "Report of the Workshop on Velocity Coupling," *Proceedings of 17th JANNAF Combustion Meeting*, Langley, Va., CPIA Pub. 324, Nov. 1980, pp. 195-210.

[20] Price, E.W. and Dehority, G.L., "Velocity Coupled Axial Mode Combustion Instability in Solid Propellant Rocket Motors," *Proceedings of 2nd ICRPG/AIAA Solid Propulsion Meeting*, Anaheim, Calif., 1967, pp. 213-227.

[21] Culick, F.E.C., "Stability of Longitudinal Oscillations with Pressure and Velocity Coupling in a Solid Propellant Rocket," *Combustion Science and Technology*, Vol. 2, No. 4, 1970, pp. 179-201.

[22] Levine, J.N. and Culick, F.E.C., "Numerical Analysis of Nonlinear Longitudinal Combustion Instability," *Metallized Propellant Solid Rocket Motors, Vol. I: Analysis and Results*, AFRPL-TR-72-88, July 1972.

[23] Lengelle', G., "A Model Describing the Velocity Response of Composite Propellants," *AIAA Journal*, Vol. 13, 1975, pp. 315-322.

[24] Condon, J.A., "A Model for the Velocity Coupling Response of Composite Propellants," Presented at the 16th JANNAF Combustion Meeting, Monterey, Calif., Dec. 1979.

[25] Srivastava, R., "Investigation of Chemically Reacting Boundary Layers in Solid Propellant Rockets: Steady and Periodic Solutions," Ph.D. Thesis, Georgia Institute of Technology, Atlanta, Feb. 1977.

[26] Beddini, R.A., "Effects of Grain Port Flow on Solid Propellant Erosive Burning," AIAA Paper 78-977, July 1978.

[27] Flandro, G.A., "Solid Propellant Acoustic Admittance Correlations," *Journal of Sound and Vibration*, Vol. 36, No. 3, 1974, pp. 297-312.

[28] Lovine, R.L., "Standardized Stability Prediction Method for Solid Rocket Motors," Vol. 1, AFRPL-TR-76-32, May 1976.

[29] Levine, J.N. and Baum, J.D., "Nonlinear Velocity Coupled Instability in Solid Rocket Motors," *Proceedings of 18th JANNAF Combustion Meeting*, Pasadena, Calif., CPIA Pub. 347, Oct. 1981, pp. 39-48.

[30] Medvedev, Yu. I. and Revyagin, L.L., "Unsteady Erosion of a Powder," *Fizika Goreniya i Vzryva*, Vol. 10, May-June 1974, pp. 341-345.